JACS
JOURNAL OF THE AMERICAN CHEMICAL SOCIETY
Article
pubs.acs.org/JACS

Co-reactant-on-Demand ECL: Electrogenerated Chemiluminescence by the in Situ Production of $S_2O_8^{2-}$ at Boron-Doped Diamond Electrodes

Irkham,[†] Takeshi Watanabe,[†] Andrea Fiorani,[‡] Giovanni Valenti,[‡] Francesco Paolucci,*[,‡] and Yasuaki Einaga*[,†,§]

[†]Department of Chemistry, Keio University, 3−14−1 Hiyoshi, Yokohama 223−8522, Japan
[‡]Department of Chemistry "G. Ciamician", University of Bologna, Via Selmi, 2, 40126 Bologna, Italy
[§]JST-ACCEL, 3−14−1 Hiyoshi, Yokohama 223−8522, Japan

Supporting Information

ABSTRACT: A novel *co-reactant-free* electrogenerated chemiluminescence (ECL) system is developed where $Ru(bpy)_3^{2+}$ emission is obtained on boron-doped diamond (BDD) electrodes. The method exploits the unique ability of BDD to operate at very high oxidation potential in aqueous solutions and to promote the conversion of inert SO_4^{2-} into the reactive co-reactant $S_2O_8^{2-}$. This novel procedure is rather straightforward, not requiring any particular electrode geometry, and since the co-reactant is only generated in situ, the interference with biological samples is minimized. The underlying mechanism is similar to that of the $Ru(bpy)_3^{2+}/S_2O_8^{2-}$ system; however, the intensity of the emitted signal increases linearly with $[SO_4^{2-}]$ up to ∼0.6 M, with possible implications for analytical uses of the proposed procedure.

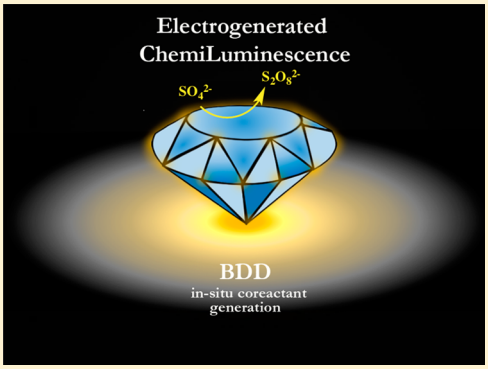

INTRODUCTION

Electrogenerated chemiluminescence (ECL) is a redox-induced light emission in which species generated at electrodes undergo high-energy electron transfer reaction to form light emitting excited states.[1−5] The development of the so-called co-reactant approach was a crucial point for the implementation of ECL as analytical technique since it permits exploitation of the technique in environmentally benign and user-friendly aqueous solutions. In fact the majority of commercially available ECL-based instruments employ this strategy.[5−7] According to the annihilation procedure, the excited state is generated by the reaction occurring at the electrode between radicals ensuing from the same species (i.e., the fluorophore),[8] whereas in co-reactant ECL, the excited state is generated through the reaction between two different precursors, the fluorophore (often $Ru(bpy)_3^{2+}$, although alternative fluorophores are currently thoroughly investigated[9−11]) and the *co-reactant*, whose electrochemical oxidation (or reduction) is first carried out. One of the most popular co-reactants for $Ru(bpy)_3^{2+}$ is tri-*n*-propylamine (TPA),[12−17] the $Ru(bpy)_3^{2+}$/TPA system being in fact at the basis of commercial ECL immunoassay and DNA analysis devices.[15]

Despite its great efficiency in generating ECL in biocompatible environments, TPA shows some disadvantages such as toxicity, high vapor pressure, and low solubility in aqueous solutions.[2] Relatively high co-reactant concentrations are usually needed in order to obtain high emission, and this may represent a severe drawback in some bioanalytical applications, where the existence of high concentrations of co-reactant species can interfere with the target biochemical analyte.[18] Notice that, in some applications, the addition of TPA is not needed, since its role is played by the analyte itself, generally an amine, for example, sarcosine,[19] dopamine,[20] NADH,[21] or other organic compounds.[22,23] Furthermore, opportunely modified fluorophores may also limit the need for added TPA, such as in recently reported ruthenium(II) complexes carrying Schiff base cavities. Due to the electrochemical oxidation of phenolic hydroxyl groups and the resonant structure of imino radicals, electrons are transferred intramolecularly to the Ru(III) center leading to the efficient generation of the Ru(II)-based excited state.[24]

In order to maintain a more general analytical applicability, the *in situ generation of co-reactant* starting from a relatively unreactive precursor would represent a promising alternative approach capable to keep the great advantages typical of such a highly sensitive technique. At the same time, it would allow one to circumvent most of the aforementioned drawbacks such as toxicity issues and interference with the biomolecules. In such a context, peroxydisulfate ($S_2O_8^{2-}$) offers some advantages with respect to amines. $S_2O_8^{2-}$ has widely been used as a co-reactant in many ECL applications[25−27] where, upon cathodic

Received: August 28, 2016
Published: November 4, 2016

DOI: 10.1021/jacs.6b09020
J. Am. Chem. Soc. 2016, 138, 15636−15641

reduction, it forms the sulfate radical anion ($SO_4^{\bullet-}$), a strongly oxidizing intermediate.[25,28] It has been shown that the ECL efficiency for the $Ru(bpy)_3^{2+}/S_2O_8^{2-}$ is about half that of the annihilation system.[26] Besides being coupled to common luminophores such as Ru complexes, luminol, and their derivatives, peroxydisulfate was also shown to exhibit ECL behavior at magnesium, silver, and platinum electrodes, where dissolved oxygen can react with $SO_4^{\bullet-}$, thus generating light-emitting species such as $^1O_2$, $^1(^1O_2)_2$, and $^3(^1O_2)_2$.[29] Several examples based on such an approach have recently been reported, such as a label-free and highly sensitive ECL aptasensor for kanamycin,[30] also coupled to nanocarbons,[31] quantum dots,[32] and gold nanoclusters[33,34] for the high sensitivity detection of chemicals,[35] antigens,[36] and nucleic acids.[37,38] Importantly, peroxydisulfates are commercially prepared by the electrolytic oxidation of aqueous solutions of sulfate precursors, for example, ammonium sulfate with platinum or platinized titanium anodes at high current densities. Therefore, the in situ electrogeneration of peroxydisulfate represents a viable strategy to obtain a co-reactant-free ECL system. In fact, the co-reactant would be generated, at will and in situ, by applying a suitably positive potential in a solution containing the sulfate precursor followed by the step to negative potential that can ignite the ECL emission. Notice that a similar procedure would not be accessible in the case of amines. Given the very high potential required to perform the anodic oxidation of sulfate to peroxydisulfate (E° = 2.01 V vs SHE), anode materials displaying very high overpotentials for the oxygen evolution reaction are however needed for the efficient production of peroxydisulfates. Boron-doped diamond (BDD) is known for its wider potential window compared to conventional electrodes, such as glassy carbon or metals (platinum, gold).[39,40] In particular, BDD has been proposed as anode to perform the efficient oxidization of SO_4^{2-} into peroxydisulfate,[41,42] and it has been used for the development of laboratory devices for the determination of sulfates and peroxydisulfates, adapted for the online monitoring in process control applications.[43]

Moreover, in recent years, BDD has also been proposed as electrode material for ECL, in particular in applications using $Ru(bpy)_3^{2+}$ with either TPA[16,17,44,45] or alcohols and ethers[39] or finally with luminol.[46]

Herein we report on a *co-reactant-free ECL system* (Figure 1) in which the unique ability of BDD (i) to promote peroxydisulfate generation with high efficiency is coupled with (ii) the high overpotential for the hydrogen evolution reaction obtained at the same electrode to allow, in the end, the efficient ECL generation in a $Ru(bpy)_3^{2+}/SO_4^{2-}$ aqueous solution. The procedure is rather straightforward, not requiring any particular electrode geometry, and since the reactive co-reactant $S_2O_8^{2-}$ is only generated on the electrode surface for a short time, the interference with biological samples is minimized.

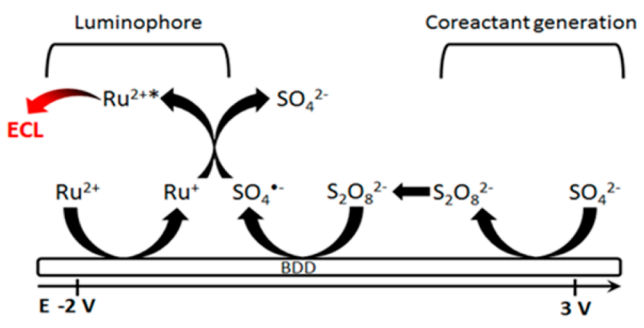

Figure 1. Reaction mechanism of electrochemiluminescence generation from $Ru(bpy)_3^{2+}$ on BDD electrode with sulfate ions. Ru = $Ru(bpy)_3$.

EXPERIMENTAL SECTION

Materials. All reagents were obtained commercially and used without further purification. $Ru(bpy)_3Cl_2$ $6H_2O$, Na_2SO_4, $Na_2S_2O_8$, and $KClO_4$ were obtained from Sigma-Aldrich. Pure water was doubly distilled with maximum conductivity 18 MΩ obtained from Simply-Lab water system (DIRECT-Q 3 UV, Millipore).

Preparation of BDD. The BDD films were deposited on a silicon(111) wafer by using a microwave plasma-assisted chemical vapor deposition (MPCVD) system (CORNES Technologies/ASTeX−5400). Acetone and trimethoxyborane were used as the source of carbon and boron, respectively, with atomic ratio of B/C = 1%. The surface morphology of the BDD was examined with field emission scanning electron microscope (FESEM, JEOL JSM-7600F). Raman spectra were recorded with an Acton SP2500 (Princeton Instruments) with excitation at 532 nm from a green laser diode in ambient temperature.

Electrochemiluminescence Measurement. All ECL measurements were conducted in a conventional three electrode system in a PTFE cell with 1% BDD, platinum spiral, and Ag/AgCl (saturated KCl) as working, counter, and reference electrodes, respectively, with PGSTAT302 (AUTOLAB Instrument).

The ECL signal was measured with a photomultiplier tube (PMT, Hamamatsu R4220p) placed in constant distance inside a dark box. A voltage of 750−800 V was supplied to the PMT. The light/current/voltage curves were recorded by collecting the preamplified PMT output signal (by an ultralow-noise Acton research model 181) with the second input channel of the ADC module of the AUTOLAB instrument. For measuring the origin of the light, a voltage of 800 V was supplied to the PMT, and the light was measured directly without amplification. Stabilizing the surface of the BDD electrode was carried out before each measurement by electrochemical cleaning by performing 10 voltammetric cycles between −3.0 and 3.0 V followed by 10 cycles between 0 and −3.0 V in 0.1 M $KClO_4$ solution with scan rate 0.3 V/s (XPS characterization before and after the electrochemical treatment is reported in Figure S1).

RESULTS AND DISCUSSION

The BDD used for the electrochemical and ECL measurements showed a typical Raman spectrum for highly boron-doped diamond, exhibiting a zone-center phonon line observed as a shoulder peak around 1300 cm^{-1}. (Figure 2a).[47] The SEM image of the BDD showed that the predominant facet having a 3-fold symmetry axis is the (111) facet, which is known as a more electrochemically active domain than the (100) facet (Figure 2b).[44]

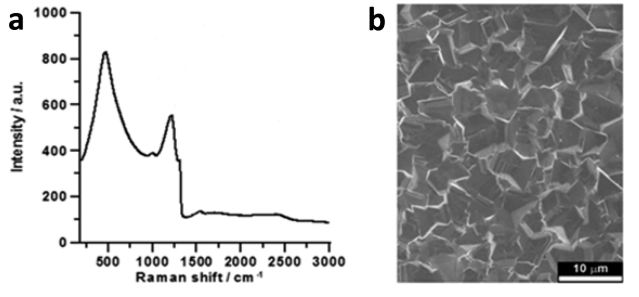

Figure 2. (a) Raman spectrum and (b) SEM image of 1% BDD.

DOI: 10.1021/jacs.6b09020
J. Am. Chem. Soc. 2016, 138, 15636−15641

The electrochemical and the ECL properties of $Ru(bpy)_3^{2+}$ in 0.1 M Na_2SO_4 aqueous solution on BDD electrodes were first investigated by cyclic voltammetry (CV). Figure 3 displays

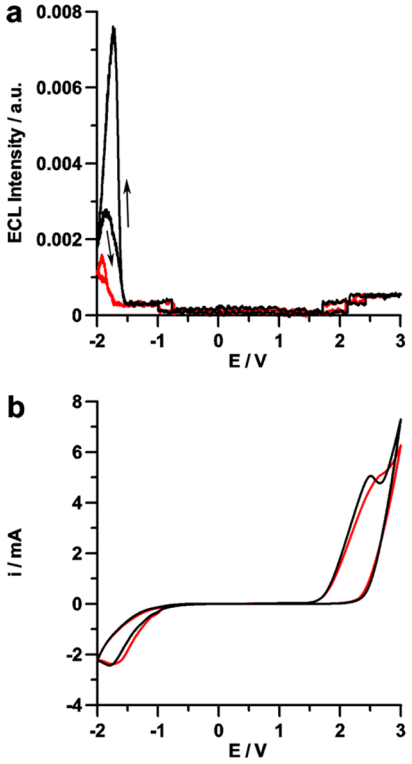

Figure 3. (a) ECL and (b) CV comparison between 0.1 M Na_2SO_4 (black) and 0.1 M $KClO_4$ (red) measurement of 5 μM $Ru(bpy)_3Cl_2$ in water solvent. Scan rate 100 mV/s, potential referred to Ag/AgCl (KCl sat) at room temperature. PMT bias 750 V.

the ECL-potential curves (a) and the corresponding CV curves (b) obtained by scanning the potential initially from 0 to 3.0 V followed by a scan to negative potentials (−2.0 V).

The first positive scan is meant to generate, at the BDD electrode surface, a sufficiently high concentration of peroxydisufate ions (eq 1) to fuel the ECL emission process during the negative potential scan, according to the following general mechanism (all the potential are reported vs Ag/AgCl):

positive potential scan

$$2SO_4^{2-} \rightarrow S_2O_8^{2-} + 2e^- \qquad E^\circ = 1.81\ V \tag{1}$$

negative potential scan

$$S_2O_8^{2-} + e^- \rightarrow SO_4^{\bullet-} + SO_4^{2-} \qquad E^\circ = 0.40\ V \tag{2}$$

$$Ru(bpy)_3^{2+} + e^- \rightarrow Ru(bpy)_3^{+} \qquad E^\circ = -1.48\ V \tag{3}$$

$$Ru(bpy)_3^{+} + S_2O_8^{2-} \rightarrow Ru(bpy)_3^{2+} + SO_4^{\bullet-} + SO_4^{2-} \tag{4}$$

$$Ru(bpy)_3^{+} + SO_4^{\bullet-} \rightarrow Ru(bpy)_3^{2+*} + SO_4^{2-} \tag{5}$$

$$Ru(bpy)_3^{2+*} \rightarrow Ru(bpy)_3^{2+} + h\nu \tag{6}$$

As shown in Figure 3a (black line), during the voltammetric cycle in 0.1 M aqueous Na_2SO_4, ECL was efficiently generated at $E^\circ \leq -1.5$ V, that is, in the region where reduction of both peroxydisulfate (reaction 2) and $[Ru(bpy)_3]^{2+}$ (reaction 3) may take place, thus making the sequence of processes outlined by eqs 4−6 possible. Notice that, according to the established mechanism depicted above,[26] peroxydisulfate may be reduced to generate sulfate anion radical, either directly at the electrode (eq 2) or by mediation of $Ru(bpy)_3^{+}$ (eq 4). The profile of ECL emission vs potential is similar to that obtained in the $Ru(bpy)_3^{2+}/S_2O_8^{2-}$system (Figure S2), thus substantiating the above hypothesis that $S_2O_8^{2-}$co-reactant is effectively produced at the BDD electrode during the first scan at positive potentials. In line with the above hypothesis, an intense ECL signal was only observed when potential was swept in the first scan to sufficiently high values, that is, where the electrogeneration of peroxydisulfate occurs (Figure S3).

CV in 0.1 M aqueous Na_2SO_4 (Figure 3b, black line) shows the broad and intense peak in the first scan at 2.5 V, indicating electrogeneration of peroxydisulfate. On the other hand, the CV curve obtained in the absence of sulfate ions, that is, in 0.1 M aqueous $KClO_4$ (Figure 3b, red line) also shows a comparable oxidation peak in similar potentials with somewhat duller shape. Such a peak prior to intense oxygen evolution reaction (OER) is often observed at BDD electrodes. It is reported that this pre-OER peak is related to a water oxidation reaction to generate hydroxyl radical (eq 7) via the surface redox couple of BDD.[48]

$$H_2O \rightarrow OH^\bullet + H^+ + e^- \qquad E^\circ = 2.52\ V \tag{7}$$

Hydroxyl radicals are considered to weakly interact with surface of BDD so that eq 7 is formally written as

$$BDD + H_2O \rightarrow BDD(OH^\bullet) + H^+ + e^- \tag{8}$$

where BDD represents the active site on the electrode surface. This reaction 8 may occur at slightly negative potential to E° for eq 7 due to the weak interaction to the surface of BDD. Kapalka et al. reported that the pre-OER peak attributed to eq 8 was observed from 1.8 to 2.4 V vs Ag/AgCl in 1 M $HClO_4$ aqueous solution.[48] Furthermore, Khamis et al. reported that in the pre-OER potential domain, an indirect oxidation process for generation of peroxydisulfate can occur via surface mediated reaction with $BDD(OH^\bullet)$ as shown in following equations:[41]

$$BDD(OH^\bullet) + SO_4^{2-} \rightarrow BDD(SO_4^{\bullet-}) + OH^- \tag{9}$$

$$BDD(SO_4^{\bullet-}) + SO_4^{2-} \rightarrow BDD + S_2O_8^{2-} + e^- \tag{10}$$

where the surface site $BDD(SO_4^{\bullet-})$ is not as oxidative as $SO_4^{\bullet-}$ but is sufficient to lead to the generation of peroxydisulfate according to the overall mechanism depicted in eq 1.[41] In the case of perchlorate solution, the oxidation current observed at pre-OER potential domain is considered as generation of oxygen (eq 11) following reaction 8[48]

$$BDD(OH^\bullet) \rightarrow BDD + 1/2O_2 + H^+ + e^- \tag{11}$$

In Na_2SO_4 aqueous solutions, this reaction 11 also occurs in the pre-OER potential domain as competing reaction with eq 9. Actually, the CVs conducted in N_2-bubbled 0.1 M Na_2SO_4 showed an ORR peak in cathodic scan after sweeping to 2.5 V (Figure S4). Thus, considering the E° value and similar oxidation current in the pre-OER potential domain in both Na_2SO_4 and $KClO_4$ solutions, the water discharge reaction (eq 8) is not fast and rate-determining step around the pre-OER potential domain, that is, around peak potential. Accordingly, in our experiment, it is considered that peroxydisulfate is mainly

DOI: 10.1021/jacs.6b09020
J. Am. Chem. Soc. 2016, 138, 15636−15641

generated by indirect oxidation process through the reactions 8, 9, and 10.

In cathodic scan, the large reduction peak observed starting around −1.0 V in both solutions, Na_2SO_4 and $KClO_4$, is mainly due to oxygen reduction reaction (ORR) since oxygen can be produced in the first positive scan (see Figure S4). The reductions of both peroxydisulfate (reaction 2) and $[Ru(bpy)_3]^{2+}$ (reaction 3) were considered to be masked with this ORR peak. Despite the occurrence of the ORR, a massive hydrogen evolution reaction (HER) that would more greatly inhibit the process leading to ECL at very negative potentials could be avoided because of choosing Na_2SO_4 instead of H_2SO_4 or $NaHSO_4$, as precursor of electrogenerated peroxydisulfate.

Furthermore, BDD is uniquely suited to promote ECL emission under such conditions, since parallel experiments carried out with either Pt or glassy carbon electrodes were unsuccessful (Figure S5); at such electrodes, water oxidation proceeds via a different route and even if hydroxyl radicals can be produced, the radicals would react with the electrodes themselves rather than the sulfate ions.

Importantly, the ECL spectrum (Figure 4), recorded during chronoamperometric experiments (vide infra), shows a maximum wavelength at 609 nm, which is expectedly in full agreement with the attribution of the emitted light to the $Ru(bpy)_3^{2+}$ based excited state and excluding that other potential emitters, such as oxygen, may be playing an important role in the observed phenomenon.[26]

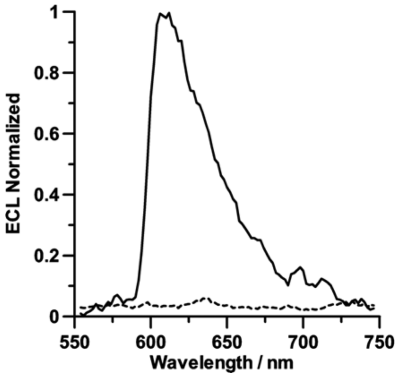

Figure 4. Normalized ECL spectrum of 5 μM $Ru(bpy)_3Cl_2$/0.1 M Na_2SO_4 system (solid line) and 5 μM $Ru(bpy)_3Cl_2$/0.1 M $KClO_4$ system (dashed line) in aqueous solution. PMT bias 800 V.

Interestingly, a weak emission was also obtained when potential was swept in the first scan up to 1.5 V, that is, at potentials too low to produce peroxydisulfate but sufficiently high to oxidize the $Ru(bpy)_3^{2+}$ fluorophore ($E°$ = 1.02 V vs Ag/AgCl, see Figure S3, inset). A possible explanation for such a weak emission is therefore that, in the present system, ECL generation may also take place according to the annihilation route (eq 12), where $Ru(bpy)_3^{3+}$ generated in the first (positive) scan may react with $Ru(bpy)_3^{+}$ generated in the second (negative) one:[49]

$$Ru(bpy)_3^{+} + Ru(bpy)_3^{3+} \rightarrow Ru(bpy)_3^{2+*} + Ru(bpy)_3^{2+} \quad (12)$$

Such a mechanism, which involves the couple of fluorophores in either their oxidized or reduced form, is generally unobserved in aqueous media where the prevailing HER prevents formation of the reduced species $Ru(bpy)_3^{+}$,[26] while it would be made possible in the present case by the high overpotential for HER on BDD. In line with such a hypothesis, Figure 3a (red line) shows the ECL-potential plot obtained in 0.1 M $KClO_4$ solutions, that is, in the absence of sulfate ions, displaying a noticeable, although very weak signal associated with reaction 12. Notice that annihilation ECL for aqueous $Ru(bpy)_3^{2+}$ solutions was only previously reported in the case of interdigitated carbon microelectrode arrays, with 2 μm width spacing, working in a generation/collection biasing mode.[50] In the present case, instead, annihilation ECL would be obtained from $Ru(bpy)_3^{2+}$ aqueous solutions only by virtue of the unique properties of BDD electrodes, without requiring any particular geometry of the cell and electrode system.

Further insight in the underlying mechanism, and quantification, of the ECL emission in the present system was obtained by performing chronoamperometric experiments where potential was first stepped from 0 to 3.0 V, where it was kept for various time durations (t_{ox}) to generate variable amounts of co-reactant, and then to −2.0 V to ignite the ECL process (see Figure 5b, inset); the current (Figure S6) and ECL light (Figure 5b) signals were continuously monitored. While the current curves decrease monotonically, the ECL signal exhibits a steep increase after each complete oxidation−

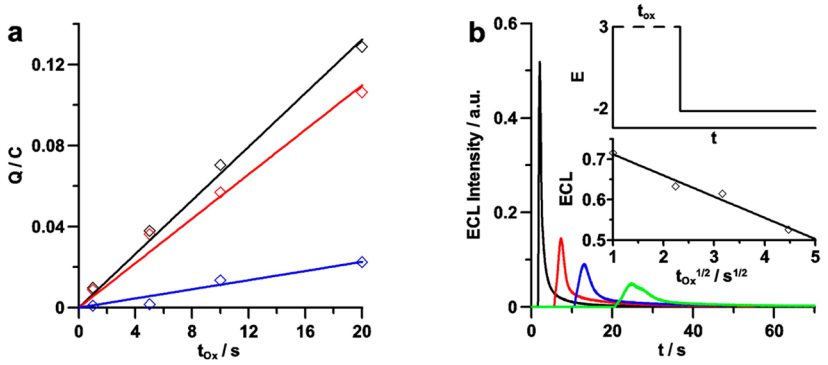

Figure 5. (a) Integrated charge at 3.0 V for different oxidation times for 0.1 M Na_2SO_4 (black), 0.1 M $KClO_4$ (red), and the differences (blue) and (b) ECL intensity transients measured during chronoamperometric experiments carried out in a 5 μM $Ru(bpy)_3Cl_2$ and 0.1 M Na_2SO_4 aqueous solution; first step from 0 to 3.0 V for t_{ox} = 1, 5, 10, or 20 s, followed by a step to −2.0 V for 50 s. The ECL transients are displaced along the time scale according to the increasing of the oxidation step duration (t_{ox}). Figure b, inset: (top) potential program used in the chronoamperometric experiments; (bottom) integrated ECL intensity vs square root of time step duration t_{ox}. PMT bias 750 V.

DOI: 10.1021/jacs.6b09020
J. Am. Chem. Soc. 2016, 138, 15636−15641

reduction cycle, followed by a rapid decay, reflecting the complex sequence of processes described by eqs 1−6 involving the production and encounter of the reacting species in the diffusion layer. Oxidation currents measured in the first step, in either the presence or absence of sulfate ions, were integrated and were found to increase linearly with the oxidation time, t_{ox} (Figure 5a), thus suggesting that formation of the surface reactive species (eq 8), rather than diffusion of the sulfate precursor, controls the oxidation current in the present conditions. By contrast, the integrated ECL signals (measured during the step at −2.0 V) decrease linearly with the square root of t_{ox} (Figure 5b, inset) indicating that the efficiency of the overall ECL generation process is limited by diffusion of sulfate precursor to the electrode and of electrogenerated peroxydisulfate toward the bulk of solution.

The efficiency of ECL generation was finally investigated at various sulfate concentrations. Current efficiency for sulfuric acid oxidation to peroxydisulfuric acid has been reported to increase with H_2SO_4 concentration.[51] In the present case, the efficiency of peroxydisulfate electrogeneration was in fact found to increase linearly with $[SO_4^{2-}]$ up to ∼0.6 M and then deviate negatively at higher concentrations (Figure S7), that is, at significantly lower concentration than the reported maximum current efficiency for peroxydisulfate electrogeneration, obtained with sulfuric acid concentration ≥2 M.[51] Importantly, deviations from linearity of the ECL signal as a function of sulfate concentration (in the range 10^{-3} to 1 M, Figure 6), occurred at significantly lower values than those observed for current, since the signal, following an initial linear increase (up to 0.1 M), reaches a plateau at $[SO_4^{2-}] \approx 0.5$ M. A similar trend was also observed in the ECL efficiency (i.e., after normalization by the $S_2O_8^{2-}$ amount, see Figure S8).

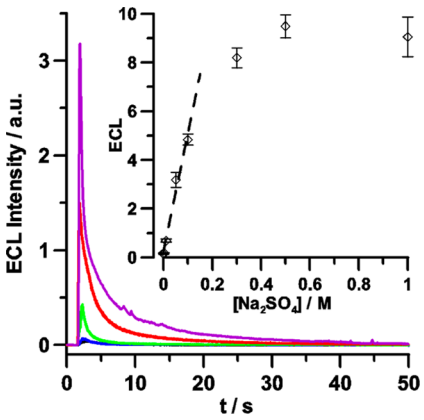

Figure 6. ECL intensity transient at various Na_2SO_4 concentrations in 5 μM $Ru(bpy)_3Cl_2$ aqueous solutions; first step 3.0 V for 1 s, followed by a step to −2.0 V for 50 s. Na_2SO_4: 1 mM (blue), 10 mM (green), 0.1 M (red), 1 M (purple), and 0.1 M $KClO_4$ (black), Inset: integrated ECL intensity as a function of concentration. PMT bias 750 V.

The observed trend of ECL intensity vs sulfate precursor concentration can tentatively be ascribed to the known ability of peroxydisulfate ion to effectively quench the excited state $Ru(bpy)_3^{2+*}$.[26] It has been reported that the ECL intensity of the $Ru(bpy)_3^{2+}/S_2O_8^{2-}$ system is in fact a function of $S_2O_8^{2-}$ concentration with a maximum emission at $[S_2O_8^{2-}] \approx 15-20$ mM.[26] The dependence of the ECL intensity vs $[SO_4^{2-}]$ observed in the present case would therefore reflect the increasing competition, as the sulfate ion concentration increases, between the two processes associated with the electrogenerated peroxydisulfate, one leading to a more efficient ECL production (through an increased rate of peroxydisulfate generation) and the other to a faster quenching of the excited state.[52,53]

Finally, analytical applications of the present system can be envisaged within the observed linearity range (1−100 mM). BDD electrodes were proposed for the detection and measurement of sulfate ions, with detection limits in the grams per liter range (∼10 mM), through their anodic oxidation to peroxydisulfate followed by the amperometric detection of peroxydisulfate (eq 2), and some commercial development has been proposed.[43,54] In such a context, the present ECL-based approach would therefore allow one to reach detection limits for sulfate ions in the millimolar range, that is, at least 1 order of magnitude lower than the reported amperometric method.

CONCLUSIONS

The generation of ECL from aqueous solutions containing the $Ru(bpy)_3^{2+}$ fluorophore and SO_4^{2-} was reported for the first time. The underlying mechanism is similar to that of the $Ru(bpy)_3^{2+}/S_2O_8^{2-}$ system, except that in this case $S_2O_8^{2-}$ is electrogenerated in situ from the sulfate precursor, exploiting the unique ability of BDD electrodes to promote electrochemical reactions with compounds that have highly positive standard potentials. The intensity of the emitted signal was found to increase linearly with $[SO_4^{2-}]$ up to ∼0.6 M, thus opening possible analytical uses of the present approach with detection limits for sulfate ions as low as 1 mM. Finally, evidence was also found of ECL emission generated by $Ru(bpy)_3^{2+}$ through the annihilation mechanism, an unprecedented result in aqueous solutions that would also be associated with the wide potential windows achievable with BDD.

ASSOCIATED CONTENT

Supporting Information

The Supporting Information is available free of charge on the ACS Publications website at DOI: 10.1021/jacs.6b09020.

XPS analysis of pretreated BDD, ECL emission in acetonitrile, ECL emission at different scanned potential, cyclic voltammetry in deaerated solution, effect of different electrode materials, effect of oxidation time, integrated anodic charge as a function of Na_2SO_4 concentration, and ECL efficiency as function of the SO_4^{2-}. (PDF)

AUTHOR INFORMATION

Corresponding Authors

*einaga@chem.keio.ac.jp

*Francesco.paolucci@unibo.it

ORCID

Giovanni Valenti: 0000-0002-6223-2072

Notes

The authors declare no competing financial interest.

ACKNOWLEDGMENTS

We thank the University of Bologna, Italian Ministero dell'Istruzione, Università e Ricerca (MIUR-project PRIN 2010), and FARB, Fondazione Cassa di Risparmio in Bologna.

DOI: 10.1021/jacs.6b09020
J. Am. Chem. Soc. 2016, 138, 15636−15641

Irkham acknowledges INPEX SCHOLARSHIP FOUNDATION.

REFERENCES

(1) *Electrogenerated Chemiluminescence*; Bard, A. J., Ed.; Marcel Dekker: New York, 2004.
(2) Richter, M. M. *Chem. Rev.* **2004**, *104*, 3003.
(3) Forster, R. J.; Bertoncello, P.; Keyes, T. E. *Annu. Rev. Anal. Chem.* **2009**, *2*, 359.
(4) Hu, L.; Xu, G. *Chem. Soc. Rev.* **2010**, *39* (8), 3275.
(5) Hesari, M.; Ding, Z. *J. Electrochem. Soc.* **2016**, *163* (4), H3116.
(6) Miao, W. *Chem. Rev.* **2008**, *108*, 2506.
(7) Liu, Z.; Qi, W.; Xu, G. *Chem. Soc. Rev.* **2015**, *44* (10), 3117.
(8) Valenti, G.; Fiorani, A.; Di Motta, S.; Bergamini, G.; Gingras, M.; Ceroni, P.; Negri, F.; Paolucci, F.; Marcaccio, M. *Chem. - Eur. J.* **2015**, *21* (7), 2936.
(9) Kerr, E.; Doeven, E. H.; Barbante, G. J.; Hogan, C. F.; Hayne, D. J.; Donnelly, P. S.; Francis, P. S. *Chem. Sci.* **2016**, *7*, 5271.
(10) Zhou, Y.; Gao, H.; Wang, X.; Qi, H. *Inorg. Chem.* **2015**, *54* (4), 1446.
(11) Della Ciana, L.; Zanarini, S.; Perciaccante, R.; Marzocchi, E.; Valenti, G. *J. Phys. Chem. C* **2010**, *114* (8), 3653.
(12) Deaver, D. R. *Nature* **1995**, *377*, 758−760.
(13) Leland, J. K. *J. Electrochem. Soc.* **1990**, *137* (10), 3127.
(14) Noffsinger, J. B.; Danielson, N. D. *Anal. Chem.* **1987**, *59*, 865.
(15) Miao, W.; Choi, J. P.; Bard, A. J. *J. Am. Chem. Soc.* **2002**, *124* (48), 14478.
(16) Yang, Y.; Oh, J. W.; Kim, Y. R.; Terashima, C.; Fujishima, a; Kim, J. S.; Kim, H. *Chem. Commun.* **2010**, *46* (31), 5793.
(17) Honda, K.; Yoshimura, M.; Rao, T. N.; Fujishima, a. *J. Phys. Chem. B* **2003**, *107* (7), 1653.
(18) Xu, J.; Huang, P.; Qin, Y.; Jiang, D.; Chen, H. *Anal. Chem.* **2016**, *88* (9), 4609.
(19) Valenti, G.; Rampazzo, E.; Biavardi, E.; Villani, E.; Fracasso, G.; Marcaccio, M.; Bertani, F.; Ramarli, D.; Dalcanale, E.; Paolucci, F.; Prodi, L. *Faraday Discuss.* **2015**, *185*, 299.
(20) Stewart, A. J.; Hendry, J.; Dennany, L. *Anal. Chem.* **2015**, *87* (23), 11847.
(21) De Poulpiquet, A.; Diez-Buitrago, B.; Dumont Milutinovic, M.; Sentic, M.; Arbault, S.; Bouffier, L.; Kuhn, A.; Sojic, N. *Anal. Chem.* **2016**, *88*, 6585.
(22) Yuan, Y.; Han, S.; Hu, L.; Parveen, S.; Xu, G. *Electrochim. Acta* **2012**, *82*, 484.
(23) Kebede, N.; Francis, P. S.; Barbante, G. J.; Hogan, C. F. *Analyst* **2015**, *140* (21), 7142.
(24) Li, P.; Jin, Z.; Zhao, M.; Xu, Y.; Guo, Y.; Xiao, D. *Dalton Trans.* **2015**, *44* (5), 2208.
(25) Bolleta, F.; Ciano, M.; Balzani, V.; Serpone, N. *Inorg. Chim. Acta* **1982**, *62* (C), 207.
(26) White, H. S.; Bard, A. J. *J. Am. Chem. Soc.* **1982**, *104* (25), 6891.
(27) Ege, D.; Becker, W. G.; Bard, a J. *Anal. Chem.* **1984**, *56* (13), 2413.
(28) Memming, R. *J. Electrochem. Soc.* **1969**, *116* (6), 785.
(29) Reshetnyak, O. V.; Koval'chuk, E. P. *Electrochim. Acta* **1998**, *43*, 465.
(30) Zhao, M.; Zhuo, Y.; Chai, Y. Q.; Yuan, R. *Biomaterials* **2015**, *52* (1), 476.
(31) Wu, L.; Wang, J.; Ren, J.; Li, W.; Qu, X. *Chem. Commun. (Cambridge, U. K.)* **2013**, *49* (50), 5675.
(32) Liang, J.; Yang, S.; Luo, S.; Liu, C.; Tang, Y. *Microchim. Acta* **2014**, *181* (7−8), 759.
(33) Hesari, M.; Workentin, M. S.; Ding, Z. *ACS Nano* **2014**, *8* (8), 8543.
(34) Wang, T.; Wang, D.; Padelford, J. W.; Jiang, J.; Wang, G. *J. Am. Chem. Soc.* **2016**, *138* (20), 6380.
(35) Yuan, D.; Chen, S.; Yuan, R.; Zhang, J.; Zhang, W. *Analyst* **2013**, *138* (20), 6001.
(36) Zhang, F.; Mao, L.; Zhu, M. *Microchim. Acta* **2014**, *181* (11−12), 1285.
(37) Cheng, Y.; Lei, J.; Chen, Y.; Ju, H. *Biosens. Bioelectron.* **2014**, *51*, 431.
(38) Sun, H.; Ma, S.; Li, Y.; Qi, H.; Ning, X.; Zheng, J. *Biosens. Bioelectron.* **2016**, *79*, 92.
(39) Honda, K.; Yamaguchi, Y.; Yamanaka, Y.; Yoshimatsu, M.; Fukuda, Y.; Fujishima, A. *Electrochim. Acta* **2005**, *51*, 588.
(40) Yamanaka, Y.; Miyamoto, M.; Tanaka, Y.; Nagumo, a.; Katsuki, Y.; Fukuda, Y.; Yoshimatsu, M.; Takeshige, a.; Kondo, T.; Fujishima, a.; Honda, K. *Electrochim. Acta* **2008**, *53* (16), 5397.
(41) Khamis, D.; Mahé, E.; Dardoize, F.; Devilliers, D. *J. Appl. Electrochem.* **2010**, *40* (10), 1829.
(42) Hippauf, F.; Dorfler, S.; Zedlitz, R.; Vater, A.; Kaskel, S. *Electrochim. Acta* **2014**, *147*, 589.
(43) Provent, C.; Haenni, W.; Santoli, E.; Rychen, P. *Electrochim. Acta* **2004**, *49*, 3737.
(44) Honda, K.; Noda, T.; Yoshimura, M.; Nakagawa, K.; Fujishima, A. *J. Phys. Chem. B* **2004**, *108*, 16117.
(45) Sentic, M.; Virgilio, F.; Zanut, A.; Manojlovic, D.; Arbault, S.; Tormen, M.; Sojic, N.; Ugo, P. *Anal. Bioanal. Chem.* **2016**, *408* (25), 7085.
(46) Garcia-Segura, S.; Centellas, F.; Brillas, E. *J. Phys. Chem. C* **2012**, *116* (29), 15500.
(47) Watanabe, T.; Honda, Y.; Kanda, K.; Einaga, Y. *Phys. Status Solidi A* **2014**, *211* (12), 2709.
(48) Kapałka, A.; Fóti, G.; Comninellis, C. *Electrochim. Acta* **2007**, *53* (4), 1954.
(49) Tokel, N. E.; Bard, A. J. *J. Am. Chem. Soc.* **1972**, *94* (8), 2862.
(50) Fiaccabrino, G. C.; Koudelka-Hep, M.; Hsueh, Y. T.; Collins, S. D.; Smith, R. L. *Anal. Chem.* **1998**, *70* (19), 4157.
(51) Serrano, K.; Michaud, P. a.; Comninellis, C.; Savall, a. *Electrochim. Acta* **2002**, *48* (4), 431.
(52) White, H. S.; Becker, W. G.; Bard, A. J. *J. Phys. Chem.* **1984**, *88* (9), 1840.
(53) Lewandowska-Andralojc, a.; Polyansky, D. E. *J. Phys. Chem. A* **2013**, *117* (40), 10311.
(54) http://www.neocoat.ch (accessed June 28, 2016).

DOI: 10.1021/jacs.6b09020
J. Am. Chem. Soc. 2016, 138, 15636−15641